

Review

Synthesis and photosensitizing properties of conjugated polymers that contain chlorotricarbonyl bis(phenylimino)acenaphthene rhenium(I) complexes

Wai Kin Chan^{a,*}, Ching Sum Hui^a, Ka Yan Kitty Man^a, Kai Wing Cheng^a,
Hei Ling Wong^a, Nianyong Zhu^a, Aleksandra B. Djurišić^b

^a Department of Chemistry, The University of Hong Kong, Pokfulam Road, Hong Kong, China

^b Department of Physics, The University of Hong Kong, Pokfulam Road, Hong Kong, China

Received 26 July 2004; accepted 22 October 2004

Available online 21 December 2004

Contents

1. Introduction	1352
2. Experimental	1352
2.1. Materials	1352
2.1.1. Complex 1	1352
2.1.2. Complex 2a	1352
2.1.3. Complex 2b	1353
2.2. Polymerization reaction	1353
3. Results and discussion	1353
3.1. Synthesis and characterizations of model compounds	1353
3.2. Syntheses and characterization of polymers	1356
3.3. Photosensitizing properties of polymers	1357
4. Conclusions	1358
Acknowledgements	1358
References	1358

Abstract

A series of poly(*p*-phenylenevinylene)s that contain chlorotricarbonyl bis(phenylimino)acenaphthene rhenium(I) complexes on the conjugated main chain was synthesized by the palladium catalyzed coupling reaction. The chloride ligand could be displaced by the iodide generated in situ during the polymerization reaction. The ligand displacement reaction was studied by synthesizing two model compounds, whose structures were confirmed by X-ray crystallography. The metal content in the polymers could be adjusted by varying the monomer feed ratio in the polymerization. The photosensitizing properties of these metal-containing polymers were studied, and it was found that the photocurrent response was dependent on the metal content in the polymers. Multilayered photovoltaic devices were fabricated, and their properties were studied by irradiation with simulated solar light. Typical power conversion efficiencies for these devices were measured to be 0.06%, with a fill factor of approximately 0.2.

© 2004 Elsevier B.V. All rights reserved.

Keywords: Conjugated polymers; Photovoltaic; Rhenium

* Corresponding author. Tel.: +852 2859 8943; fax: +852 2857 1586.

E-mail address: waichan@hku.hk (W.K. Chan).

1. Introduction

The chemistry and photophysics of chlorotricarbonyl rhenium(I) diimine complexes has been studied extensively because of their potential applications as photosensitizers, emission sensitizers, photooxidants, and photocatalysts [1]. These complexes possess relatively long-lived excited states which are of metal-to-ligand charge transfer (MLCT) character; they have been incorporated into a variety of π -conjugated oligomeric or polymeric systems [2]. Our group has been continuously investigating the uses of molecular [3] and polymeric [4] rhenium diimine complexes as potential photosensitizers or light emitters. We have synthesized a series of rhenium complexes based on 1,4-diaza-1,3-butadiene (DAB) that can function as photosensitizers in simple, two-layer photovoltaic devices [5]. Compared to molecular metal complexes, these metal-containing polymers enjoy the advantages that they have better processibility and can form optical quality thin films easily by spin casting technique. In addition, the excited state properties of the metal containing polymers can also be fine-tuned by adjusting their metal content, or by modifying the π -conjugated main chain/ligands coordinated to the metal centre. More recently, we found that a chlorotricarbonyl rhenium(I) complex based on bis(phenylimino)acenaphthene (DIAN) ligand can be processed into thin film by vacuum sublimation. The complex is non-emissive due to the presence of a relatively low-lying MLCT excited state. The bulk heterojunction photovoltaic device fabricated from this complex exhibited a power conversion efficiency of 0.48% with a fill factor of 0.56 [6]. In this paper, we describe the synthesis and characterization of a series of poly(p-phenylenevinylene)s (PPV) incorporated with this rhenium DIAN complex on the polymer main chain. It was also found that during the polymerization, the axial chloride ligand could be displaced by the iodide ligand generated in situ, which was studied in detail. The potential of using these rhenium complexes containing polymer as photosensitizer was investigated. A series of multilayer photovoltaic devices was fabricated and their photocurrent response was measured.

2. Experimental

2.1. Materials

DMF was distilled over CaH_2 under reduced pressure. Unless otherwise specified, all chemicals were used as received.

Instrument. NMR spectra were recorded on a Bruker DPX-300 (300 MHz) NMR spectrometer. Chemical shifts were reported in ppm and tetramethylsilane (TMS) was used as the internal standard. IR spectra were recorded as KBr disc on a Bio-Rad FTS-71R spectrometer. UV–vis absorption spectra were collected with a Hewlett-Packard 8452A photodiode array spectrometer. Positive ion EI and FAB mass spectra were collected on a Finnigan MAT95 mass spectrometer. Crystal-

lographic data were collected on a Rigaku AFC7R four-circle diffractometer equipped with graphite monochromator coupled with a RU 200 rotating anode generator, with the molybdenum anode operating at 160 mA and 50 kV. Data collection was carried out on Marresearch Imaging Plate mar300 without equipment for absorption correction, therefore, no absorption correction was carried out on both compounds. The structures were solved by direct methods (SIR-97) [7] and refined with all data on F^2 by the least square method using SHELXL-97 [8].

2.1.1. Complex 1

The ligand used in the synthesis of complex **1** was synthesized according to the procedure reported in the literature [9]. A mixture of 4-iodoaniline (3.56 g, 22.0 mmol), acenaphthenequinone (2.0 g, 11.0 mmol) and anhydrous zinc chloride (1.8 g, 13.2 mmol) in glacial acetic acid (20 mL) was refluxed for 30 min. The suspension was cooled to room temperature and the solid was filtered. It was washed with acetic acid (2×10 mL) and diethyl ether (4×20 mL) and then air-dried. The orange colored zinc complex obtained was added to an aqueous solution of potassium carbonate (25 g in 25 mL water) and the mixture was heated under reflux with rigorous stirring. After 2 h the mixture was cooled to room temperature, and the solid was filtered off and washed thoroughly with water. After recrystallization with ethanol, the ligand was used immediately for the subsequent reaction. A mixture of the ligand (0.20 g, 0.35 mmol) and rhenium pentacarbonyl chloride (0.14 g, 0.39 mmol) was refluxed in toluene under a nitrogen atmosphere for 3 h. After the solution was cooled, the dark purple precipitate was filtered. The solid was dissolved in chloroform and reprecipitated in ether. Yield: 0.28 g (94%). ^1H NMR (CDCl_3): δ 8.11 (*d*, $J = 8.3$ Hz, 2H), 7.96 (*d*, $J = 8.7$ Hz, 4H), 7.54 (*t*, $J = 7.4$ Hz, 2H), 7.48 (*d*, $J = 6.5$ Hz, 2H), 7.10 (*m*, 4H). ^{13}C NMR (CDCl_3): δ 195.4, 173.1, 148.3, 145.1, 139.6, 139.1, 131.6, 128.8, 125.9, 125.9, 125.0, 123.4, 93.7. FTIR (KBr pellet): $\nu = 2019, 1922, 1887\text{ cm}^{-1}$. UV–vis (CHCl_3). EI–MS: m/z : 890 (M^+), 855 ($\text{M}^+ - \text{Cl}$). Anal. Calc. for $\text{C}_{27}\text{H}_{17}\text{N}_2\text{O}_3\text{Cl}_{12}\text{Re}$: Calc.: C, 36.3; H, 1.9; N, 3.1. Found: C, 35.9; H, 2.2; N, 3.0%.

2.1.2. Complex 2a

A mixture of complex **1** (16.1 mg, 0.018 mmol), styrene (23.6 mg, 0.18 mmol), palladium(II) acetate (2 mg, 0.009 mmol), lithium chloride (7.6 mg, 0.18 mmol), and tri-*n*-butylamine (0.10 g) was heated in DMF (3 mL) under a nitrogen atmosphere at 80 °C for 2 days. The mixture was poured in water and the crude product collected was purified by column chromatography using chloroform/hexane (1:1) as the eluent. Yield: 33 mg (41%). ^1H NMR (acetone- d_6): δ 7.28 (*d*, $J = 8.0$ Hz, 2H), 7.33 (*m*, 2H), 7.43 (*t*, $J = 8.0$ Hz, 4H), 7.45 (*m*, 4H), 7.60 (*m*, 2H), 7.71 (*m*, 8H), 7.97 (*d*, $J = 8.2$ Hz, 4H), 8.34 (*d*, $J = 8.2$ Hz, 2H). Anal. Calc. for $\text{C}_{43}\text{H}_{28}\text{N}_2\text{O}_3\text{ClRe}$: Calc.: C, 61.3; H, 3.3; N, 3.3. Found: C, 60.7; H, 3.2; N, 3.0%.

2.1.3. Complex **2b**

Complex **2b** was prepared by the same procedure as in the synthesis of **2a**, except that no LiCl was added. Yield: 29%. ^1H NMR (acetone- d_6): δ 7.26 (d, $J=8.2$ Hz, 2H), 7.31 (m, 2H), 7.43 (t, $J=8.2$ Hz, 4H), 7.46 (m, 4H), 7.60 (m, 2H), 7.71 (m, 6H), 7.90 (m, 2H), 7.96 (d, $J=8.0$ Hz, 4H), 8.32 (d, $J=8.0$ Hz, 2H). Anal. Calc. for $\text{C}_{43}\text{H}_{28}\text{N}_2\text{O}_3\text{Ir}$: Calc.: C, 55.3; H, 3.0; N, 3.0. Found: C, 55.8; H, 3.3; N, 2.6%.

2.2. Polymerization reaction

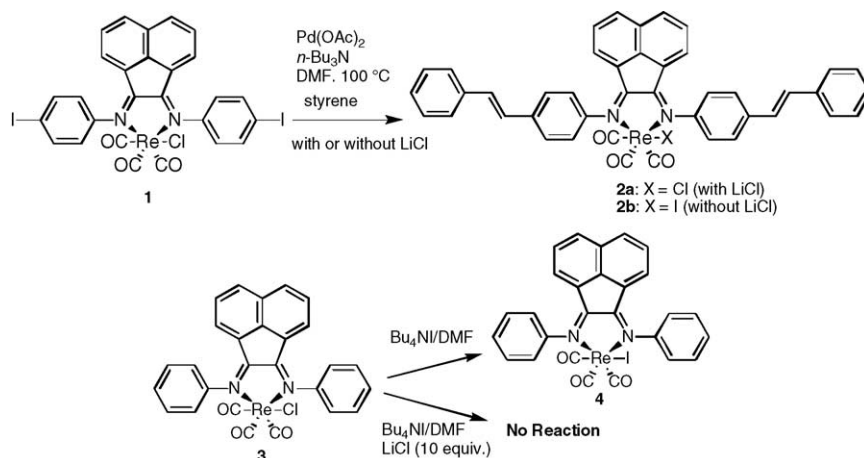
The synthesis of polymer **5a** is described as the general procedure. Complex **1** (0.10 g, 0.11 mmol), 2,5-dihexoxy-1,4-diiodobenzene (0.55 g, 1.03 mmol), *p*-divinylbenzene (0.15 g, 1.15 mmol), palladium(II) acetate (0.01 g, 0.06 mmol), tri-*o*-tolylphosphine (0.018 g, 0.06 mmol) and lithium chloride (0.49 g, 11.5 mmol) were introduced into a 50 mL Schlenk flask under a nitrogen atmosphere. Anhydrous DMF (3 mL) and tri-*n*-butylamine (0.64 g, 3.45 mmol) were then added via a syringe to the mixture. The solution was stirred at 100 °C for 7 days. The reaction mixture was poured into methanol and a dark green solid was collected by filtration. The polymer was washed with methanol in a Soxhlet extractor for 2 days and dried under vacuum for 2 days. Yield: 70%. FTIR (KBr), cm^{-1} : $\nu=2023, 1926, 1906$ (facial carbonyl CO stretching), UV–vis (CHCl_3): λ_{max} : 458 nm.

3. Results and discussion

3.1. Synthesis and characterizations of model compounds

In our attempt to polymerize $\text{Re}(\text{DIAN-I})(\text{CO})_3\text{Cl}$ [DIAN-I = bis(*p*-iodophenylimino)acenaphthene] **1** with divinylbenzene by the Heck reaction, we found that the chloride ligand at the rhenium centre was replaced by an iodide

ligand, which was formed in situ during the palladium catalyzed reaction. This was confirmed by the synthesis of model compound **2b** by the reaction between **1** and styrene in the presence of palladium catalyst (Scheme 1). Complex **2b** was obtained in 41% yield, and no chloro substituted rhenium complex was found. We also found that the ligand displacement reaction was suppressed in the presence of excess chloride ligand. When the reaction was carried out in large excess of LiCl (10 equiv.), complex **2a** was obtained instead. The ligand displacement reaction could also be carried out in different solvents including DMF, dioxane, THF, and *m*-cresol with similar results obtained. The importance of the presence of free iodide in the reaction medium was examined by another model reaction in which complex **3** reacted with 2 equivalent of Bu_4NI in DMF (Scheme 1), which yielded the iodo complex **4** in 40% yield. When 10 equiv. of Bu_4NI was used in the reaction, the yield was slightly improved to 55%. This ligand displacement reaction can also be suppressed in the presence of excess chloride ligand. No complex **4** was formed when **3** was treated with a mixture of Bu_4NI and 10-fold excess of LiCl. Based on these observations, a simple ligand displacement reaction is proposed. In other reports, the displacement of chloride ligand was observed in $\text{Re}(2,2'\text{-bpy})(\text{CO})_3\text{Cl}$ (2,2'-bpy = 2,2'-bipyridine) in the formation of complexes with Re–Re or Re–Mn bonds [10]. It was suggested that the metal–metal bond was not formed via a simple nucleophilic attack mechanism but involved prior electron transfer to generate $[\text{Re}(\text{CO})_3\text{bpyCl}]^{\bullet-}$, which subsequently lost a Cl^- and formed a new Re–metal bond. Such reactions can only occur in those complexes that are easily reduced. In another paper, it was reported that the ligand displacement reaction could occur electrochemically [11]. Reduced complexes such as $[\text{Re}(\text{CO})_3(\alpha\text{-diimine})\text{Br}]^{\bullet-}$ were generated electrochemically, which subsequently reacted with a better π accepting ligand (e.g. PPh_3) to form $[\text{Re}(\text{CO})_3(\alpha\text{-diimine})\text{PPh}_3]^+$. The one electron reduction of $[\text{Re}(\text{CO})_3(\alpha\text{-diimine})\text{L}]$ would lead to the formation $[\text{Re}_2(\text{CO})_6(\alpha\text{-diimine})_2]$ or $[\text{Re}(\text{CO})_3(\alpha\text{-diimine})\text{L}]^{\bullet-}$,



Scheme 1. Synthesis of complexes **2a** and **2b**.

depending on the nature of L and the π -accepting ability of the diimine ligand. In our case, both complexes **2a** and **2b** exhibit very similar and relatively low reduction potentials [$E_{1/2} = -1.02$ V (versus Ag/AgCl) for complex **2a**] because of the relatively lower π^* level in the DIAN ligands than other diimine ligands [12]. Therefore, we cannot rule out that the formation of $[\text{Re}(\text{CO})_3(\text{diimine})\text{Cl}]^{\bullet-}$ was the first step of the reaction in which iodide may act as the reductant. This is followed by the displacement of chloride by the iodide ligand. We also attempted to prepare a bromo complex using Bu_4NBr . However, the product yield was very low ($\sim 5\%$), which was consistent with π donating abilities of the halide ligands. In $\text{Re}(\text{diimine})(\text{CO})_3\text{X}$ type complexes, changing the axial halide ligand from Cl to I will change not only the excited state energy but also the excited state character. Compared to chlorotricarbonyl complexes, there were fewer reports concerning the synthesis and properties of bromo or iodo complexes [13]. In fact, bromotricarbonyl rhenium(I) diimine complexes are common starting materials for the synthesis of the corresponding metal alkyls [14]. The bromo and iodo complexes were usually synthesized by the reaction between diimine ligand and rhenium pentacarbonyl bromide and iodide, respectively. To the best of our knowl-

edge, no inter conversion between the halide complexes was reported.

The structures of both model complexes were unambiguously confirmed by X-ray crystallography in which the halide ligands were clearly identified [15]. Fig. 1 shows the X-ray crystal structures of complexes **2a** and **2b**, and their crystallographic data are summarized in Table 1. Both complexes take up slightly distorted octahedral geometries that are almost identical except the halide ligands. However, the crystal systems of these two complexes are not the same, showing the influence of the size of the halide ligand to the crystal packing. There is a significant difference in the $\text{Re}-\text{C}(1)$ bond lengths in complexes **2a** (2.116 Å) and **2b** (2.036 Å). In addition, the difference in the $\text{C}(1)-\text{O}(1)$ bond lengths in the carbonyl trans to the halide ligand is even larger (0.960 Å in **2a** and 0.765 Å in **2b**). The unusual CO bond length in **2b** may be caused by the disorder of halide and its opposite CO ligand. However, treatment by disorder model was not successful. It is because the iodide overlaps partially with the disordered CO group and the positions of partially occupied CO group was located with unexpected small displacement.

Fig. 2 shows the electronic absorption spectra of complexes **2a–b** measured in CH_2Cl_2 . An iodide complex will

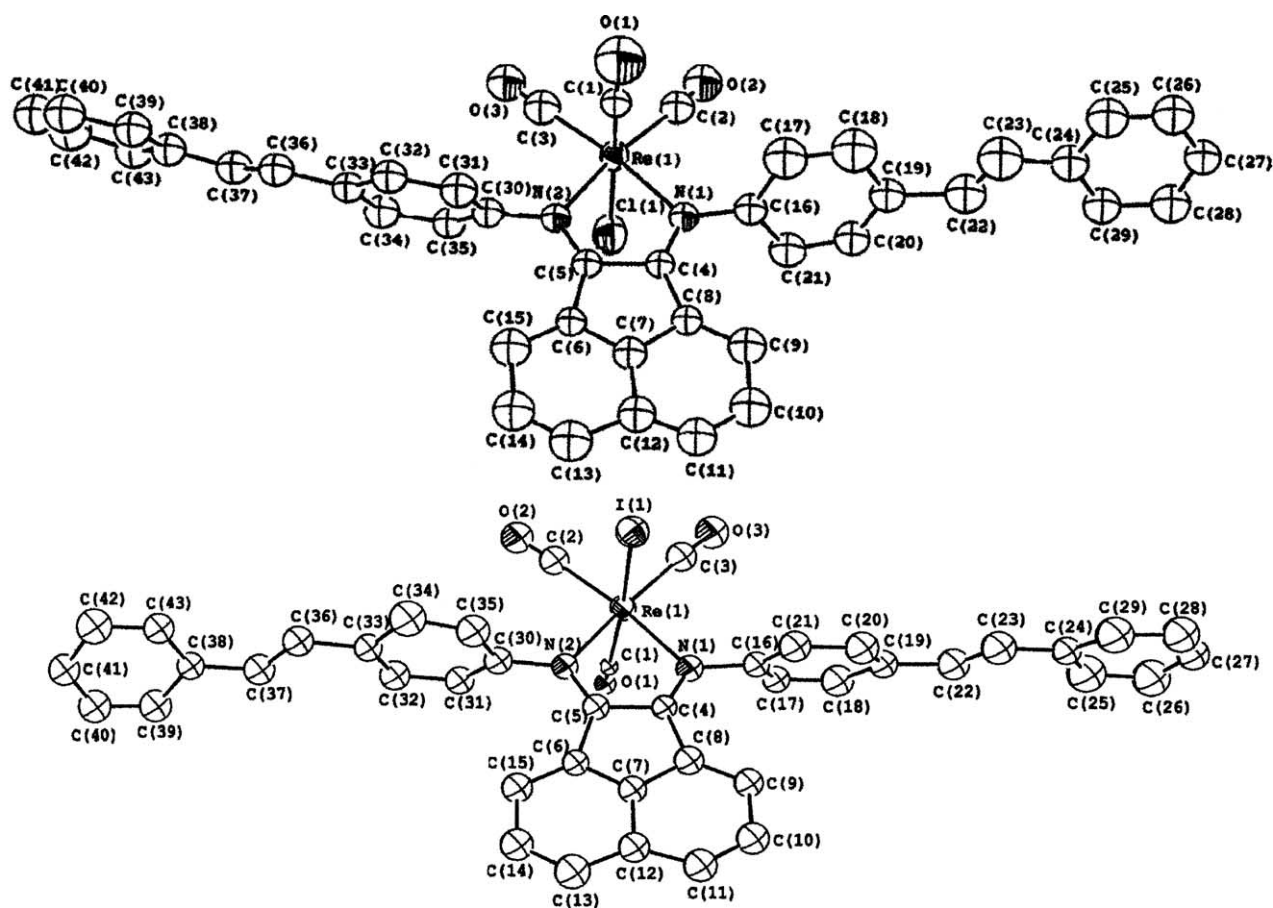


Fig. 1. Structures of complexes **2a** (top) and **2b** (bottom) showing the atomic numbering. Selected bond lengths and angles for complex **2a**: $\text{Re}(1)-\text{Cl}(1)$, 2.459(7) Å; $\text{Re}(1)-\text{C}(1)$, 2.116(12) Å; $\text{Cl}(1)-\text{Re}(1)-\text{C}(1)$, $166.4(4)^\circ$; $\text{N}(1)-\text{Re}(1)-\text{N}(2)$, $74.8(6)^\circ$. For complex **2b**: $\text{Re}(1)-\text{I}(1)$, 2.7513(18) Å; $\text{Re}(1)-\text{C}(1)$, 2.0356(10) Å; $\text{I}(1)-\text{Re}(1)-\text{C}(1)$, $173.83(5)^\circ$; $\text{N}(1)-\text{Re}(1)-\text{N}(2)$, $74.6(5)^\circ$.

Table 1
Crystallographic data for complexes **2a** and **2b**

	2a	2b
Empirical formula	C ₄₃ H ₂₈ N ₂ O ₃ ClRe	C ₄₃ H ₂₈ N ₂ O ₃ IRe
Formula weight	842.32	933.77
Temperature (K)	301(2)	253(2)
Crystal system	Monoclinic	Triclinic
Space group	<i>P</i> 2 ₁ / <i>n</i>	<i>P</i> 1
Unit cell dimensions		
<i>a</i> (Å)	11.607(2)	14.066(3)
<i>b</i> (Å)	33.730(7)	15.674(3)
<i>c</i> (Å)	17.941(4)	17.212(3)
α (°)	90	99.58(3)
β (°)	90.42(3)	93.12(3)
γ (°)	90	107.02(3)
<i>V</i> (Å ³)	7024(2)	3556.5(12)
<i>Z</i>	8	4
Absorption coefficient	3.579	4.328
Crystal size (mm ³)	0.2 × 0.1 × 0.06	0.3 × 0.2 × 0.1
θ Range for data collection (°)	1.29–25.52	1.21–25.33
Reflection collected	10966	14562
Independent reflections	6053	8979
Parameter	421	418
<i>wR</i> ₂ (all data)	0.1393	0.1163
<i>R</i> ₁ [<i>I</i> > 2 σ (<i>I</i>)]	0.0582	0.0499

give rise to an increased mixing between the metal d and halide p orbitals, as the p orbital energy increases from Cl to I. Therefore, the lowest excited states in iodo complex may exhibit both halide-to- α -diimine charge transfer (XLCT) and MLCT in character. Complex **2a** exhibits an intense MLCT [$d(\text{Re})-\pi^*(\text{diimine})$] transition absorption band at 495 nm, which is consistent to those reported previously [16]. On the other hand, interesting absorption features were observed in complex **2b**. Besides the MLCT band at 510 nm, another lower energy absorption band is observed at 549 nm, which is tentatively assigned to the XLCT transition [$P_\pi(\text{I})-\pi^*(\text{diimine})$]. The absorption maxima of these two electronic transitions in different solvents are summarized in Table 2. The charge transfer characters of the MLCT bands in both complexes are also supported by the neg-

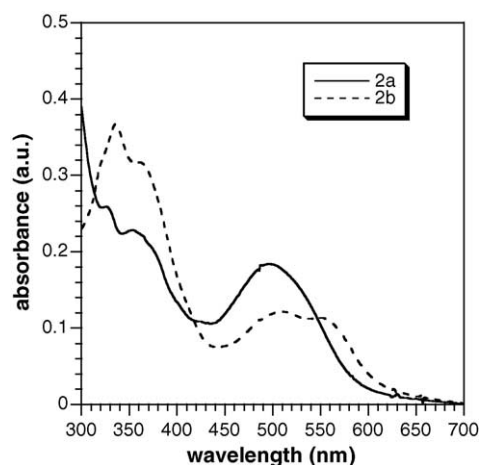


Fig. 2. UV-vis absorption spectra of complexes **2a** and **2b** in CH₂Cl₂.

Table 2
Spectroscopic properties of different complexes

Complex	λ_{max} (nm) (ϵ Lmol ⁻¹ cm ⁻¹)		ΔE^{a} (cm ⁻¹)		E_{red} (V) ^b
	Toluene	CH ₂ Cl ₂	THF	DMF	
2a	519(6170)	495(11750)	505(5800)	477(8540)	-1.04
2b	578(7050), 532(6830)	549(7540), 510(8090)	562(4910), 516(5160)	540(4540), 489(5120)	-1.02

^a Difference in energy between the absorption maxima in toluene and in DMF.

^b Cyclic voltammetry experiments were performed in acetonitrile solution with 0.1 M Bu₄NPF₆ under Ar, Pt working electrode, Ag/AgCl reference.

^c Solvatochromism for the XLCT absorption band.

^d Solvatochromism for the MLCT absorption band.

Table 3
Properties of the Re-DIAN containing PPVs

Polymer	x	y	Yield (%)	T_d (°C) ^a	M_n ^b	PD ^c
5a	0.1	0.9	70	446	9200	1.9
5b	0.3	0.7	76	450	15300	2.3
5c	0.5	0.5	81	330	17200	2.5

^a Decomposition temperature determined by thermal gravimetric analyzer under a nitrogen atmosphere.

^b Number average molecular weight.

^c Polydispersity.

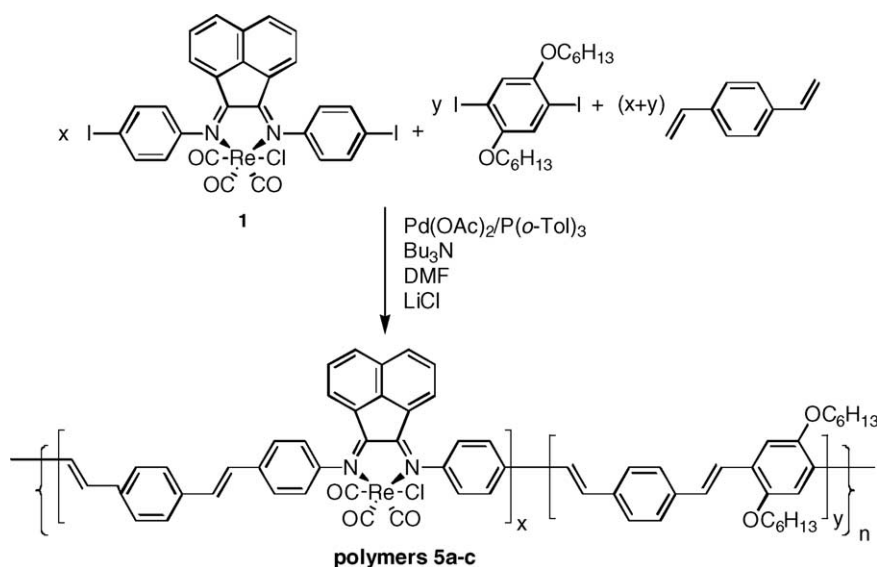
ative solvatochromism. However, for the XLCT transition band in complex **2b**, the solvent effect was found to be much weaker. Both complexes exhibit an intense absorption band at ca. 370 nm, which is assigned to the ligand-centered transition of DIAN with extended π -conjugation. In addition, for iodo and chloro complexes, the solvent polarity has little influence to this band. All these rhenium complexes are not emissive at room temperature because the non-emissive π^* (for complex **2a**) and XLCT (for complex **2b**) states may provide a more efficient non-radiative deactivation process.

3.2. Syntheses and characterization of polymers

As a result of the ligand displacement reaction observed, all subsequent polymerizations were carried in the presence of 10 equiv. LiCl. *p*-Divinylbenzene was copolymerized with different proportions of monomer **1** and 1,4-dihexoxy-2,5-diiodobenzene by the conventional Heck coupling reaction to yield polymers **5a–5c** (Scheme 2). The metal content in the resulting polymers could be adjusted by varying the ratio between different monomers. The properties of the polymers obtained are summarized in Table 3. The solubility of the polymers increased with the metal content. Polymer **5a** was not completely soluble in DMF, and it precipitated during the

course of polymerization, resulting in relatively lower yield and molecular weight. With higher metal content, polymers **5b** and **5c** show higher molecular weight, and optical quality films could be obtained by spin coating from the solution.

In the ^1H spectrum of polymer **5a**, two groups of broad peaks were found at 8.1 and 7.8 ppm, which are due to the protons on the naphthalene ring. The signals due to the protons of the PPV main chain and other protons on the naphthalene rings appeared as two broad peaks and were found at 7.2 to 7.7 ppm. Other peaks found at 4.1, 1.9, 1.2–1.4, and 0.9 ppm are attributed to the hexoxy side chain. From the protons due to the rhenium complex and the hexoxy side chain, the metal content in these copolymers can be calculated, and the experimental metal content in the copolymers agreed quite well with those of the monomer feed ratio. In the FTIR spectra of **5a–5c**, three very strong absorption bands at 2020, 1922, 1896 cm^{-1} were observed, which are assigned to the facial metal carbonyl CO stretching. This confirms the presence of rhenium carbonyl moieties in the polymer main chain. Other intense absorption bands found at 1600 cm^{-1} and 969–964 cm^{-1} are assigned to the C=N stretching bands for the diimine moiety and the out-of-plane bending of the trans vinylene group, respectively. Fig. 3 shows the UV–vis spectra of **5a–5c**. In polymer **5a**, the intense absorption peaks at ca. 450 and 370 nm are assigned to the π – π^* transition of the conjugated main chain and the DIAN ligand, respectively [17]. On the other hand, the MLCT [$d\pi$ (Re) $\rightarrow \pi^*$ (DIAN)] transition of the rhenium complex moiety only appears as a shoulder at ca. 520 nm [9]. With a higher metal content, polymer **5b** shows a more intense MLCT transition band, and the intraligand π – π^* transition at 370 nm is more obvious. When the metal content in the polymer is further increased, the intensities of the MLCT and conjugated main chain transitions become comparable. It can be observed in the absorption spectrum of polymer **5c**.



Scheme 2. Synthesis of polymers **5a–5c**.

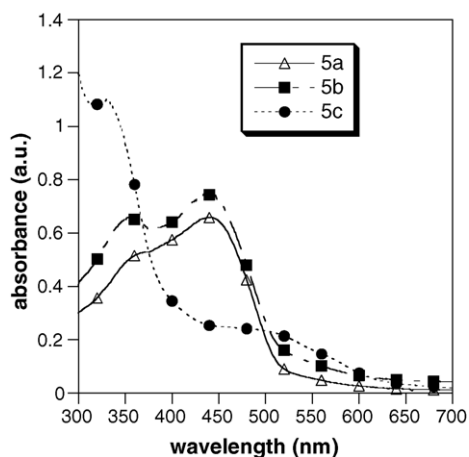


Fig. 3. UV-vis absorption spectra of polymers **5a–5c** in CHCl_3 .

3.3. Photosensitizing properties of polymers

It has previously been shown by us that ruthenium tris(2,2'-bipyridine) complex incorporated in conjugated polymers were able to act as photosensitizers [18]. In addition, the uses of ruthenium complexes in dye-sensitized solar cells with high efficiency have also been demonstrated [19]. The photosensitizing properties of these polymers were first tested by measuring their photoconductivity. The polymer films for photoconductivity measurements were prepared by casting the polymer solution in chloroform on indium tin oxide (ITO) coated glass slides. The typical thickness of the polymer film was 0.5–1 μm . Another gold electrode was coated on the polymer film surface. The photocurrent was measured with the setup as described in our previous article [20]. Argon ion laser (488 nm) was used as the light source. Optical quality films could be obtained from these polymers. Upon irradiation, an external electric field was applied across the polymer film, and the photocurrent response was measured by a lock-in amplifier. Fig. 4 shows the plots of

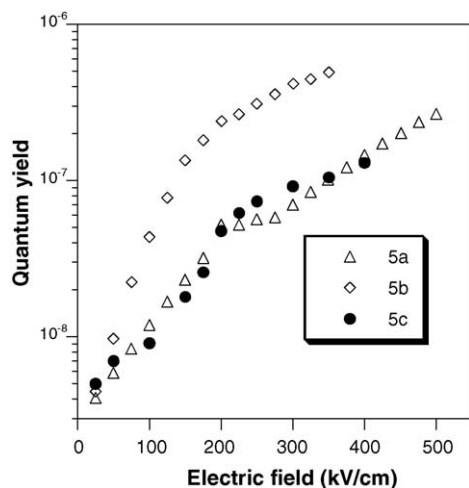


Fig. 4. Plot of quantum yield as the function of external electric field for polymers **5a–5c** upon radiation with Ar-ion laser (488 nm).

quantum yield vs. electric field strength for polymers **5a–5c**. Polymer **5b** shows higher quantum efficiency when compared to **5a**. This is explained by the higher metal complex content in the polymer. However, polymer **5c** only shows similar quantum yield to **5a** in spite of the highest metal content. It can be seen from Fig. 1 that the acenaphthene imine and the phenyl group are not coplanar. We suggest that due to the presence of the large amount of rhenium complex on the main chain, the effective conjugation length in the polymer is shortened, which subsequently affects the charge transport properties of the polymer. This clearly shows that the amount of photosensitizer content is not the sole factor that affects the photocurrent response. The presence of charge transport units (π conjugated system) is also essential.

Besides the simple single layer devices, a series of three layered photovoltaic devices based on polymers **5a–5c** with poly(3,4-ethylenedioxythiophene):poly(styrenesulfonate) (PEDOT:PSS) [21] as the hole transport layer and 3,4,9,10-perylenetetracarboxylic diimide (PTCDI) [22] as the electron-transporting layer was prepared. The photovoltaic properties of these devices were also investigated. A layer of PEDOT:PSS (25 nm) was first spin-coated on the ITO glass substrate. After spin-coating a layer of the rhenium complex containing polymer (40 nm), PTCDI (25 nm) and aluminium electrode (70 nm) were then deposited by vacuum evaporation. A 150 W Xenon lamp providing AM 1.5 simulated solar radiation (intensity = 100 mW/cm^2) was used as the light source. The current-voltage characteristics of the devices were studied with a Keithley 2400 sourcemeter. The photovoltaic properties of the devices fabricated from polymers **5a–5c** are summarized in Table 4. It was found that the device fabricated from polymer **5b** exhibited a higher power conversion efficiency ($6.1 \times 10^{-2}\%$) compared to that fabricated from polymer **5a** ($4.5 \times 10^{-2}\%$), which is due to the higher photosensitizer content. However, device fabricated from **5c** shows the lowest efficiency among these polymers. Again, we attribute this observation to the fact that both sensitizer and charge transport units are essential to the generation of photocurrent. The current-voltage characteristics of the ITO/PEDOT:PSS/DIAN-PPV **5b**/PTCDI/Al in the dark and under simulated solar light irradiation are shown in Fig. 5. The measured short-circuit current (ISC), open voltage (VOC), and fill factor (FF) were measured to be 0.42 mA/cm^2 , 0.86 V,

Table 4

Properties of the photovoltaic devices ITO/PEDOT:PSS/rhenium polymer/PTCDI/Al fabricated from polymers **5a–5c**

Polymer	I_{sc} ($\mu\text{A cm}^{-2}$) ^a	V_{OC} (V) ^b	FF ^c	η_{p} ($10^{-2}\%$) ^d
5a	37	0.93	0.21	4.5
5b	427	0.86	0.21	6.1
5c	102	0.76	0.23	1.2

^a Short-circuit current.

^b Open-circuit voltage.

^c Fill factor.

^d Power conversion efficiency.

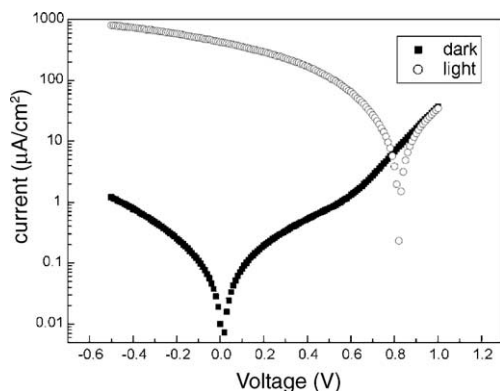


Fig. 5. Current voltage characteristics of photovoltaic devices ITO/PEDOT:PSS/polymer **5b**/PTCDI/Al under the illumination of AM 1.5 simulated solar light (100 mW/cm^2).

and 0.21, respectively. Although this device showed the best performance among these polymers, the value of FF is relatively low, which indicates slow charge transport and high recombination [23]. Therefore, it is of importance to study the detailed charge transport behavior of these polymer in order to understand the fundamentals of photovoltaic effect in these devices. We are currently extending our studies to investigate the relationship between the nature of the ligands and the photosensitivity of the rhenium complexes. Also, it is expected that improvements in the fill factor and efficiency could also be achieved by optimization of the device structure and use of bulk heterojunctions, as well as device encapsulation.

4. Conclusions

A series of conjugated polymers that contain chlorotri-carbonyl bis(phenylimino)acenaphthene rhenium(I) complex was synthesized. The chloride ligand in the rhenium complex can be displaced by the iodide ligand generated in situ in palladium catalyzed reaction, which was further confirmed by the synthesis of two different model compounds. Such ligand displacement reaction can be suppressed by adding an excess amount of lithium chloride during polymerization. The photosensitizing properties of the rhenium complex were also studied. The polymers exhibit modest photocurrent response under an external applied electric field. Photovoltaic devices were also fabricated by sandwiching the polymers between a hole transport polymer (PEDOT:PSS) and an electron transport materials (PTCDI). The devices exhibit a typical power conversion efficiency in the order of $10^{-2}\%$.

Acknowledgements

The work described in this paper was substantially supported by the grants from the Research Grants Council of the

Hong Kong Special Administrative Region, China (Project Nos. HKU 7075/01P, 7096/02P, and 7009/03P). W.K.Chan is grateful to the Outstanding Young Researcher Award and Committee on Research and Conference Grants (U of HK) for financial support.

References

- [1] K.S. Schanze, D.B. MacQueen, T.A. Perkins, L.A. Cabana, *Coord. Chem. Rev.* 94 (1994) 993.
- [2] (a) K.D. Ley, K.S. Schanze, *Coord. Chem. Rev.* 171 (1998) 287; (b) K.D. Ley, Y. Li, J.V. Johnson, D.H. Powell, K.S. Schanze, *Chem. Commun.* (1999) 1749; (c) K.A. Walters, K.D. Ley, C.S.P. Cavaleheiro, S.E. Miller, D. Gosztola, M.R. Wasielewski, A.P. Bussandri, H. van Willigen, K.S. Schanze, *J. Am. Chem. Soc.* 123 (2001) 8329.
- [3] (a) P.K. Ng, X. Gong, W.K. Chan, *Adv. Mater.* 10 (1998) 1337; (b) W.K. Chan, P.K. Ng, X. Gong, S. Hou, *Appl. Phys. Lett.* 75 (1999) 3920.
- [4] (a) W.K. Chan, P.K. Ng, X. Gong, S. Hou, *J. Mater. Chem.* 9 (1999) 2103; (b) L.S.M. Lam, S.H. Chan, W.K. Chan, *Macromol. Rapid Commun.* 21 (2000) 1081; (c) P.K. Ng, X. Gong, S.H. Chan, L.S.M. Lam, W.K. Chan, *Chem. Eur. J.* 7 (2001) 4358.
- [5] (a) L.S.M. Lam, W.K. Chan, *Chem Phys Chem.* 2 (2001) 252; (b) L.S.M. Lam, W.K. Chan, A.B. Djurišić, E.H. Li, *Chem. Phys. Lett.* 362 (2002) 130.
- [6] H.L. Wong, L.S.M. Lam, K.W. Cheng, K.Y.K. Man, W.K. Chan, C.Y. Kwong, A.B. Djurišić, *Appl. Phys. Lett.* 84 (2004) 2557.
- [7] A. Altomare, M.C. Burla, M. Camalli, G. Cascarano, C. Giacovazzo, A. Guagliardi, A.G.G. Moliterni, G. Polidori, R. Spagna, *J. Appl. Cryst.* 32 (1998) 115.
- [8] G.M. Sheldrick, *SHELXL-97* program for Crystal Structure Analysis, University of Goettingen, Germany, 1997.
- [9] G. Knör, M. Leirer, T.E. Keyes, J.G. Vos, A. Vogler, *Eur. J. Inorg. Chem.* (2000) 749.
- [10] D.L. Morse, M.S. Wrighton, *J. Organomet. Chem.* 125 (1977) 71.
- [11] G.J. Stor, F. Hartl, J.W.M. van Outersterp, D.J. Stufkens, *Organometallics* 14 (1995) 1115.
- [12] F.P.A. Johnson, M.W. George, F. Hartl, J.J. Turner, *Organometallics* 15 (1996) 3374.
- [13] (a) L.H. Staal, A. Oskam, K. Vrieze, *J. Organomet. Chem.* 170 (1979) 235; (b) E.W. Abel, V.S. Dimitrov, N.J. Long, K.G. Orrell, A.G. Osborne, H.M. Pain, V. Sik, M.B. Hursthouse, M.A. Mazid, *J. Chem. Soc., Dalton Trans.* (1993) 597; (c) B.D. Rossenaar, D.J. Stufkens, A. Vlcek Jr., *Inorg. Chem.* 35 (1996) 2902; (d) A. Gelling, K.G. Orrell, A.G. Osborne, V. Sik, M.B. Hursthouse, S.J. Coles, *J. Chem. Soc., Dalton Trans.* (1996) 203; (e) K.G. Orrell, A.G. Osborne, V. Sik, M.W. da Silva, M.B. Hursthouse, D.E. Hibbs, K.M.A. Malik, N.G. Vassilev, *J. Organomet. Chem.* 538 (1997) 171; (f) K.G. Orrell, A.G. Osbrone, M.W. da Silva, M.B. Hursthouse, S.J. Coles, *Polyhedron* 16 (1997) 3003.
- [14] (a) B.D. Rossenaar, C.J. Kleverlaan, M.C.E. van de Ven, D.J. Stufkens, A. Vlcek Jr., *Chem. Eur. J.* 2 (1996) 228; (b) C.J. Kleverlaan, D.J. Stufkens, I.P. Clark, M.W. George, J.J. Turner, D.M. Martino, H. van Willigen, A. Vlcek Jr., *J. Am. Chem. Soc.* 120 (1998) 10871; (c) C.J. Kleverlaan, D.J. Stufkens, *Inorg. Chim. Acta* 284 (1999) 61.
- [15] Crystallographic data of model complexes **2a** and **2b** have been deposited with the Cambridge Crystallographic Data Cen-

- tre, CCDC No. 198019 for complexes **2a** and 198020 for **2b**. Copies of this information may be obtained free of charge from <http://www.ccdc.cam.ac.uk/conts/retrieving.html> or the Director, CCDC, 12 union Road, Cambridge CB21EZ, UK (fax: +44 1223 336033; email: deposit @ccdc.cam.ac.uk or www: <http://www.ccdc.cam.ac.uk>).
- [16] G. Knör, M. Leirer, A. Vogler, J. Inf. Recording 24 (1998) 69.
- [17] R. van Asselt, C.J. Elsevier, W.J.J. Smeets, A.L. Spek, R. Benedix, Recl. Trav. Chim. Pays-Bas. 113 (1994) 88.
- [18] P.K. Ng, X. Gong, S.H. Chan, L.S.M. Lam, W.K. Chan, Chem. Eur. J. 7 (2000) 4358.
- [19] (a) M.K. Nazeeruddin, A. Kay, I. Rodicio, R. Humphry-Baker, E. Mueller, P. Liska, N. Vlachopoulos, M. Grätzel, J. Am. Chem. Soc. 115 (1993) 6382; (b) M.K. Nazeeruddin, P. Péchy, T. Renouard, S.M. Zakeeruddin, R. Humphry-Baker, P. Comte, P. Liska, L. Cevey, E. Costa, V. Shklover, L. Spiccia, G.B. Deacon, C.A. Bignozzi, M. Grätzel, J. Am. Chem. Soc. 123 (2001) 1613; (c) U. Bach, D. Lupo, P. Comte, J.E. Moser, F. Weissörtel, J. Salbeck, H. Spreitzer, M. Grätzel, Nature 395 (1998) 583; (d) J. Krüger, R. Plass, L. Cevey, M. Piccirelli, M. Grätzel, U. Bach, Appl. Phys. Lett. 79 (2001) 2085.
- [20] W.K. Chan, W.Y. Ng, Adv. Mater. 9 (1997) 716.
- [21] (a) A.C. Arias, M. Granström, D.S. Thomas, K. Petritsch, R.H. Friend, Phys. Rev. B 60 (1999) 1854; (b) S.A. Carter, M. Angelopoulos, S. Karg, P.J. Brock, J.C. Scott, Appl. Phys. Lett. 70 (1997) 2067; (c) J.C. Scott, S.A. Carter, S. Karg, M. Angelopoulos, Synth. Met. 85 (1997) 1197; (d) J.S. Kim, M. Granström, R.H. Friend, N. Johansson, W.R. Salaneck, R. Daik, W.J. Feast, F.C. Cacialli, J. Appl. Phys. 84 (1998) 6859.
- [22] J.-P. Meyer, D. Schlettwein, D. Wöhrle, N.I. Jaeger, Thin Solid Films. 258 (1995) 317.
- [23] J. Nelson, J. Kirkpatrick, P. Ravirajan, Phys. Rev. B 69 (2004) 035337.